The signal of sudden stratospheric warmings in surface climate

Erik Holmgren

Faculty of Science

UNIVERSITY OF GOTHENBURG

UNIVERSITY OF GOTHENBURG
Department of Earth Sciences
Geovetarcentrum/Earth Science Centre

The signal of sudden stratospheric warmings in surface climate

Erik Holmgren

Mailing address	**Address**	**Telephone**	Geovetarcentrum
Geovetarcentrum	Geovetarcentrum	031-786 19 56	Göteborg University
S 405 30 Göteborg	Guldhedsgatan 5A		S-405 30 Göteborg
			SWEDEN

Abstract

Long term conditions in the atmosphere are changing. Because of this, many of the atmospheric processes that have been studied during the last century will change. Sudden stratospheric warmings (SSWs), which occur in the polar stratosphere, are a prime example of processes that indicate the top down relationship between the stratosphere and troposphere. The frequency of SSWs is believed to change with rising temperatures. SSWs are thought to cause cold air outbreaks over the continents in the northern hemisphere, leading to potential damages to infrastructure and increased health risks.

To better understand what future atmospheric conditions infer concerning SSWs, past variations need to be understood. As of now, the record of SSWs start at 1958 due to limitations in stratospheric measurements. The goal of this thesis is to identify regions and surface climate variables sensitive to SSWs.

Spatial correlations demonstrate a positive correlation between winter temperatures and the occurrence of SSWs in northeastern North America and Africa and southern Asia. A negative connection between winter temperature and the occurrence of SSWs is displayed in northern Eurasia. A more detailed regional analysis revealed that mean winter temperatures in northeastern North America during SSW years exceeds the 10th percentile of monthly temperatures during non-SSW years. During SSW years winter mean temperatures in northern Fennoscandia are only slightly lower than during non-SSW years.

Tree ring data from northeastern North America are suggested as possible proxy data for a winter temperature reconstruction that could be used in the detection of historical SSWs.

Contents

I List of abbreviations

AO	Arctic Oscillation
a.s.l.	above sea level
CAO	Cold Air Outbreaks
EPV	Erthel's Potential Vorticity
FC	Fort Chimo
KDE	Kernel Density Estimation
KNMI	Koninklijk Nederlands Meteorologisch Instituut
MJO	Madden–Julian Oscillation
NAO	North Atlantic Oscillation
PNA	Pacific/North American Pattern
QBO	Quasi Biennial Oscillation
SK	Sodankylä
SSW	Sudden Stratospheric Warming

1 Introduction

The climate system is vast and complex with numerous interactions between the physical and chemical processes of the atmo-, bio-, cryo-, hydro-, and lithosphere. Weather is the short term result of these processes, on a longer time scale it is called climate: the statistical mean of weather. To understand climate and weather, the underlying processes and how they could be affected by small changes, need to be understood (Marshak, 2015, pp. 738-740).

The atmosphere is the layer of various gases surrounding the Earth (see Figure 1). It is divided into five parts (in order of ascending altitude): the troposphere, the stratosphere, the mesosphere, the thermosphere, and the exosphere. In this thesis, only the troposphere and stratosphere will be handled. The troposphere is the layer closest to the Earths surface, stretching from the surface to around 9–17 km a.s.l. depending on the region. The troposphere is also where the boundary layers to the other geospheres are located and hence where most of the processes affecting weather and climate are taking place. It is a turbulent layer with many processes occurring almost at random with heavy mixing of the air masses due to the negative temperature gradient. The boundary between the troposphere and stratosphere is called the tropopause (Marshak, 2015, pp. 736-738).
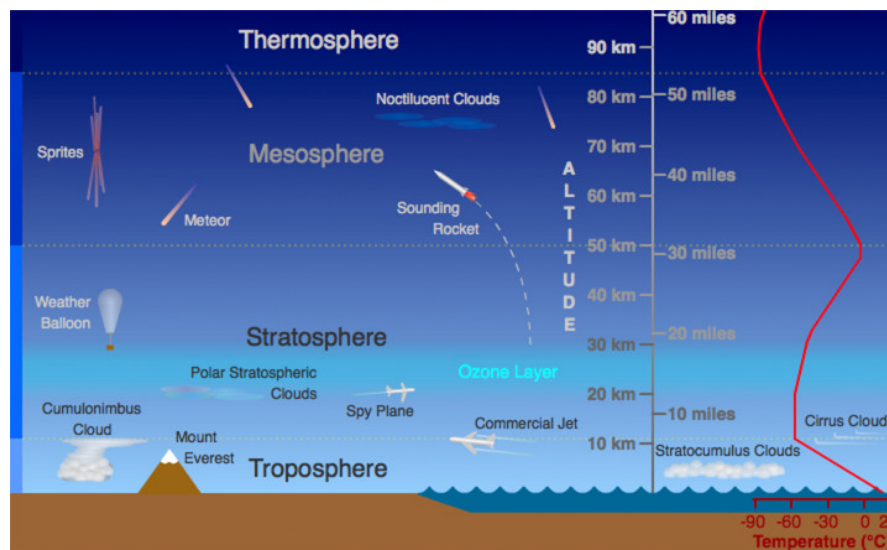

Figure 1: Structure of the atmosphere. Dotted horizontal lines indicate boundaries between the different layers. Temperature gradient is illustrated on the right side. Notice that exosphere is missing. Credit: scied.ucar.edu https://commons.wikimedia.org/wiki/File:Atmosphere_layers.jpg, https://creativecommons.org/licenses/by-sa/4.0/legalcode

The stratosphere stretches from the tropopause to around 50–60 km. It is a very stable region of the atmosphere due to the positive temperature gradient (see Figure 1). With the exception of the mixing zone close to the tropopause, where atmospheric waves propagating upwards from the troposphere break and dissipate their energy, there is almost no mixing of the air masses in the stratosphere (Stohl et al., 2003). Because of this it was for a long time believed that the slow processes

in the stratosphere wouldn't affect the state of the troposphere. It was only recently that a more dynamical coupling between the strato- and troposphere was suggested (Baldwin & Dunkerton, 2001; Thompson, Baldwin, & Wallace, 2002).

Winter circulation in the polar stratosphere is characterised by strong circumpolar winds, defined as the polar vortex. The vortex usually takes form in mid to late November when temperatures drop in the polar stratosphere due to the lack of ozone heating. This results in a negative temperature difference between the polar and mid latitude stratosphere creating the winds forming the vortex (Schoeberl, Lait, Newman, & Rosenfield, 1992). It usually lasts until late April when ozone heating raises the temperatures in the polar stratosphere, and the following reversal of the temperature gradient. Partly because of the shielding from lower latitude air masses from the strong winds, but also because of the lack of radiative heating at the poles during winter, the temperatures in the interior of the polar vortex are very low (Schoeberl & Hartmann, 1991). During its lifetime the area encompassed by the vortex can shrink and expand. Diabatic heating is affecting the stability of the air masses and increasing Erthel's potential vorticity (EPV) in the vortex while divergent winds, or frictional forces, are disturbing the vortex by peeling or diluting EPV (Nash, Newman, Rosenfield, & Schoeberl, 1996; Schoeberl et al., 1992).

1.1   Sudden stratospheric warmings

Sudden stratospheric warmings (SSWs) are examples of large scale events in the polar stratosphere where temperatures can increase ~ 30–$40°$K during the course of a few days. During certain events the climatological mean zonal westerlies present in the the winter hemisphere can change direction (Butler et al., 2015). The world meteorological association defines two types of SSWs:

- A minor SSW event occurs when a significant increase in temperature is observed on any stratospheric level anywhere in the wintertime hemisphere.

- A major SSW event occurs if the temperature gradient from $60°$N and poleward is positive and the zonal circulation has changed direction at 10 millibar or below.

When an upward propagating planetary wave reaches the critical wind line, a latitude where the magnitude of the zonal wind no longer accommodates the propagation of planetary waves, it will dissipate its energy in the form of westward acceleration. If this occurs in the polar stratosphere it will decelerate the eastward zonal winds that comprise the polar vortex. During a major SSW enough westward momentum is deposited within the polar vortex to change the direction of the zonal winds from westerly to easterly. Due to the Coriolis force this deceleration also induces a meridional motion of the air masses, which in turn results in a adiabatic temperature change. This is what raises the temperatures in the polar stratosphere during a SSW (Limpasuvan, Thompson, & Hartmann, 2004). To conclude, the rising temperatures in the polar stratosphere during a SSW is not the cause of the event, but rather a symptom of it. It is the deposition of westward momentum that causes the events (Butler et al., 2015).

Temperatures are expected to rise in coming decades (Pachauri et al., 2014). The critical wind line has been linked to atmospheric variations in the tropics, namely the quasi-biennial oscillation (QBO) (Holton & Tan, 1980) and the Madden-Julian oscillation (MJO) (Garfinkel, Feldstein, Waugh, Yoo, & Lee, 2012). The QBO is the dominating feature of equatorial stratospheric variability, consisting of downward propagating wind regimes that are either easterly or westerly depending on the phase of the oscillation (Baldwin & Dunkerton, 2001). The MJO is a planetary scale eastward movement of atmospheric circulation and convection cells in the Indian and Pacific Oceans (Zhang, 2005). Model studies have shown that rising temperatures will strengthen the MJO, and the forcing that it applies on the polar stratosphere, hence the frequency of SSWs can be expected to change in the coming years (Schimanke, Spangehl, Huebener, & Cubasch, 2013; Kang, Tziperman, Kang, & Tziperman, 2017).

SSWs are clear examples of stratospheric anomalies that can propagate downward, reaching the troposphere, and affect the weather patterns during the weeks following an event. Baldwin and Dunkerton (1999, 2001) and Limpasuvan et al. (2004) showed that large-amplitude atmospheric oscillation anomalies in the stratosphere precedes similarly sized anomalies in the troposphere, indicating a downward propagation of signatures in the stratosphere to the troposphere. This top-down relationship has shown to have an effect on tropospheric conditions and can lead to cold air outbreaks (CAOs) over the continents (Butler et al., 2015; Kolstad, Breiteig, & Scaife, 2010; Thompson et al., 2002).

CAOs have many effects on society. Storm tracks, the latitudinal extent of polar cyclones, are shown to reach lower latitudes during weak vortex periods in both the Atlantic and Pacific compared to periods of a strong vortex. This means that storms are more likely during periods of a weak polar vortex (Baldwin & Dunkerton, 2001). Severe weather can cause damages to infrastructure (Pinto, Brücher, Fink, & Krüger, 2007) and cold spells are linked to increased disease related mortality rates since brief exposure to unusually low temperatures can cause inflammatory reactions (Mercer, 2003).

1.2 The Arctic and North Atlantic Oscillation

Two important features of the climate system in the northern hemisphere are the Arctic Oscillation (AO) and the Northern Atlantic Oscillation (NAO). Both the AO and NAO are examples of the main modes of variability of geopotential height anomalies, but with different spatial extents. The AO is a zonally symmetric dipole with nodes located at the pole and around $40°–45°$N, while the NAO is centred around the North Atlantic, between Iceland and the Azores. Both the AO and NAO have well defined connections to winter time temperature and zonal winds (Fyfe, Boer, & Flato, 1999; Hurrell, 1995).

The AO index can be explained as the pressure gradient between the nodes at the Arctic and the circular mid-latitude region mentioned earlier. During periods with a strong polar vortex the cold air will be trapped in the polar region. This leads to a lower than usual geopotential and strengthens the Arctic to mid-latitude pressure gradient, resulting in a positive AO. This also coincides with

a positive phase in the NAO and higher temperatures in the sub-polar regions (NOAA, n.d.-a).

The strength of the NAO is defined as the difference between the sea-level pressure at the Icelandic low and the Azores high pressure, hence a strong NAO infers a lower than usual low pressure in Iceland and a higher than usual high pressure at the Azores. A period of high NAO is dominated by strong westerly winds across the north Atlantic resulting in milder and wetter conditions over the continents. A negative NAO has the opposite effect on surface weather (NOAA, n.d.-b). Beyond the interannual trends displayed in the NAO, longer periods of a dominant index are also occurring (Hurrell, 1995). Climate simulations have shown NAO to be relatively insensitive to atmospheric forcings, such as increased greenhouse gases, while the AO on the other hand display a positive trend when forcing is applied (Fyfe et al., 1999).

1.3 Climate reconstructions through proxies

A climate proxy is an indirect way to learn about past variations in the climate. There is a wide range of climate proxies: oxygen isotope ratios from ice cores, loess deposits, pollen concentrations in sediments and the widths of tree rings are some. They are all based on the assumption that climate will have a measurable effect on a longer lasting material. An example could be growth season temperature affecting the growth rate of a tree and thus the resulting ring width of that year. The temporal resolution of reconstructed climate variables varies from annual to seasonal depending on the proxy (Schweingruber, 1988; Bradley, 1999).

Extensive records of paleoclimatic data has become more important during the last decades due to the need of historical reference data during the development and calibration of more advanced climate models (Briffa, 2000; Mayewski et al., 2004).

1.4 Aim

To better understand how recent changes in climate might affect the future frequency of SSWs, the historic occurrences of the events has to be known. As of now, there are no documented events preceding 1958 due to the lack of stratospheric measurements before 1958. An extension of the SSW data set requires a reconstruction based on climatic variables with a longer historic record than 1958. Surface temperature, precipitation, the AO and NAO are all examples of climatic variables that have been recorded further back than 1958. Furthermore, these variables have also been reconstructed successfully using climate proxies to years long before recorded observations were made. In the quest to establish relationships between SSWs and these climatic variables, spatial correlations will be performed to identify regions of interest. Based on this a more detailed analysis will be performed on the potential regions to further understand the relationship between SSWs and surface climate.

2 Methods

The project evolves around analysis of existing data sets. A data set (see Appendix A) of all major SSWs between 1958 and 2013 was provided by Butler, Sjoberg, Seidel, and Rosenlof (2017). It lists all the major SSWs (WMO definition described earlier) found when analysing the winds at 60°N and 10hPa in the reanalysis products listed in table 1.

Table 1: Reanalysis products used in the identification of SSWs done by Butler et al. (2017).

Reanalysis	Time period	Reference	Native horizontal resolution
ERA-40	1958-2002	Uppala et al. (2005)	1.25°x1.25°
ERA-interim	1979–2014	Dee et al. (2011)	0.75°x0.75°
JRA-55	1958-2014	Kobayashi et al. (2015)	1.25°x1.25°
MERRA2	1980-2014	Molod et al. (2015)	0.5°x0.667°
NCEP-NCAR I	1958-2014	Kalnay et al. (1996)	2.5°x2.5°
NOAA20CRv2c	1958-2014	Compo et al. (2011)	2°x2°

Reanalysis products are spatially and temporally complete observational records created through the assimilation of a multitude of sources, such as surface observations and satellite data, by global coupled land-atmosphere-ocean models (Butler et al., 2017).

In the data set the SSWs were labelled with the date of the event and grouped by the year. This meant that an event in January was grouped with an event in the following December. Since SSWs occur between November and March, this was re-arranged so that a year spanned October until September, encompassing the full winter season. This also made it so that events separated by a summer wasn't counted to the same year. From this times series a winter mean (November – March) of the occurrences of SSWs was calculated.

Monthly means of the AO and NAO indices were downloaded from The Climate Prediciton Center (n.d.-a, n.d.-b). These data sets were re-sampled in a similar fashion to how the SSW data was handled, creating a year that stretched from October until September.

2.1 AO and NAO analysis

The SSW time series was correlated (Spearmans correlation) against a two month running mean of the AO and NAO time series. The two month running mean was chosen. Winter means (November – March) of AO and NAO were grouped by the occurrence of SSWs or not. The assumed normal distributions of the two groups were first checked and a kernel density function was created. To investigate how the mean values of the two groups compared, a two-sample T-test was performed. A *Levene's test* was first performed on the two groups to check the relationship between the variances. Based on this, equal variances were assumed for the two-sample T-test. The t-statistic was checked for a one- and two-tailed significance

with the assumption that the means of the two groups were equal. The mean value of each group was also checked for deviations from zero with a T-test. Based on the returned t-statistic and p-value the mean value could either be assumed not distinguished, distinguished, smaller or larger than zero.

2.2 Spatial correlations

The online tool Climate explorer from KNMI (2019) was used to perform spatial correlations between the monthly SSW series and the climate variables: temperature, precipitation, temperature anomalies and the monthly percentage of days within the 10th percentile of daily minimum temperature (TN10p). The SSW series was averaged over the months November–March, this average was then stepwise correlated to a three month moving average covering the following year for each of the climatic variables. The climatic variables were averaged over three months with the end goal of using reconstructed climate data in mind. A shorter signal would be hard to detect in reconstructed data.

Data sets used for the spatial correlations are listed in table 2. Only correlation maps with a p-field < 0.1 was selected for further analysis as this is when a statistical connection in the map is considered plausible.

Table 2: Data sets used for the spatial correlations.

Author(s)	Name	Variable	Resolution
Harris et al., 2014	CRU TS 4.01	Land temperature	0.5°
Harris et al., 2014	CRU TS 4.01	Precipitation	0.5°
Morice et al., n.d.	HadCRUT4 median	Temperature anomalies	5°
Donat et al., 2013	HadEX2	TN10p	2.5°x 3.75°

2.3 Regional analysis: Sodankylä and Fort Chimo

Based on the results from the spatial correlations a region in northeastern Canada and one in northern Finland (see Figure 2) were chosen for further analysis. Station data from Fort Chimo in Canada (58.10N, -68.40E) and Sodankylä in Finland (67.37N, 26.65E) was used to represent the monthly mean temperatures in the regions.

Figure 2: Locations of meteorological stations Fort Chimo, Canada, and Sodankylä, Finland.

Temperature data from the two sites was re-sampled into a "winter year" beginning in October and ending in September. Years were grouped according to the occurrence or no occurrence of a SSW during the winter months for both of the locations. By calculating a mean value for each month based on the years within the groups, a normalised year was created. For the normalised year the 10th and 90th percentiles were also calculated. The November – March average SSW value was correlated (Spearmans correlation) against a two month running mean of the temperature from both of the locations. For both the locations a mean winter period was created based on the months displaying the highest correlations in the previous step and was in turn correlated against the November – March average SSW value.

Based on findings in previous described steps the relationship between the two locations was further investigated by correlating (Pearsons correlation) the two month running means against each other. The November–March means was also correlated against each other.

3   Results

Combining the results from the six different reanalysis data sets yielded a total of 41 events between winter of 1958 and 2013. This equates to 0.73 events per year. The monthly distribution of events are shown in table 3. Most of the events occur in January and February, 15 and 12 events respectively. Seven events occurred in March while only two respective five events occurred in November and December.

Table 3: Monthly distribution of SSWs between 1958 and 2013 in the October–September time series created out of the data from Butler et al. (2017). Months April–October are left out since no SSWs occur during these months.

Month	Number of SSWs
November	2
December	5
January	15
February	12
March	7

3.1 AO and NAO analysis

The AO and NAO both display (see Figure 3) negative correlations to the mean winter SSW value ($p < 0.05$) during the winter months January to March, with significant correlations between AO and winter SSWs extending into April. The AO exhibits slightly stronger correlations to SSWs than the NAO during the significant periods.
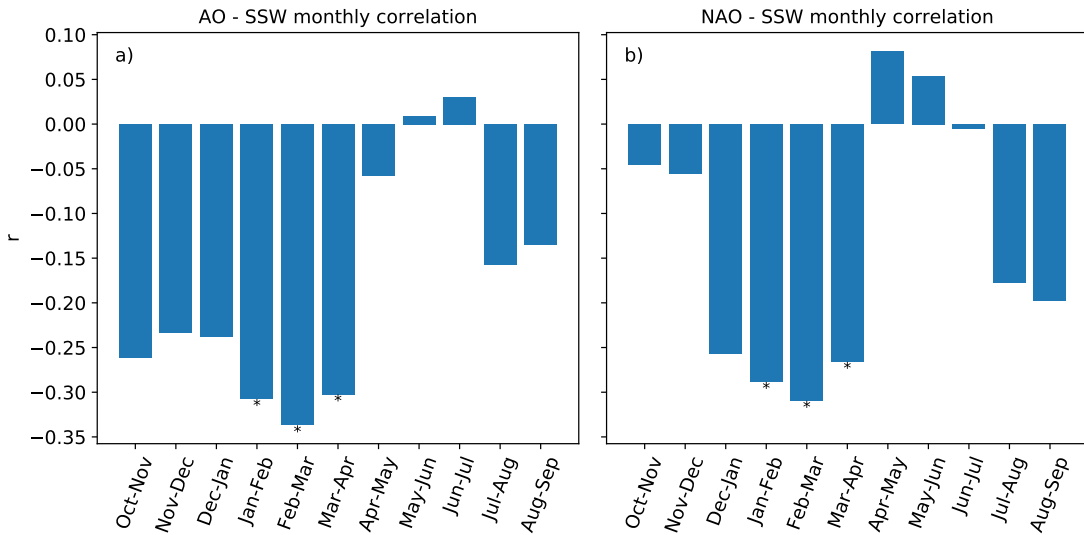

*Figure 3: Correlation statistics from correlating the November–March mean SSW value against a two month running mean AO and NAO. Period significance is indicated by *: $p < 0.05$. a) AO display significant negative correlations between January and April. b) NAO display significant negative correlations between January and April.*

The kernel density estimations (KDE) of the mean winter AO index during years with and without SSWs are displayed in figure 4a. The means of the two groups are distinguishable with the mean winter AO index during years with SSWs being significantly (p<0.05) lower than the mean winter AO during non-SSW years.
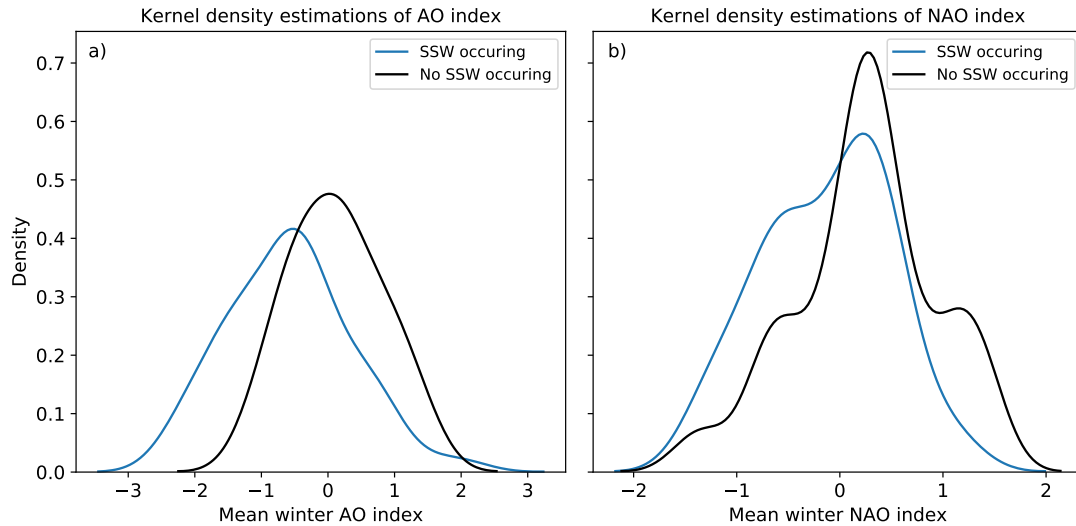
Figure 4: Kernel density estimations for: a) mean winter AO index during years with SSWs occurring in blue and years with no SSWs occuring in black. b) Mean winter NAO index during years with SSWs occurring in blue and years with no SSWs occurring in black.

Figure 4b shows the KDE of the mean winter NAO index during years with and without SSWs. The winter mean of non-SSW years is significantly larger than the winter means during SSW years. Winter means during SSW years is not significantly distinguishable from zero.

3.2 Spatial correlation maps

The spatial correlations indicated significant ($p<0.05$) relationships between the occurrence of SSWs during the winter months and temperature in certain regions. Correlations between SSWs and the average temperature in January-March exhibit (see Figure 5) coherent regions with positive relationships in northeastern North America, northeastern Africa and southern Asia. Regions of negative relationships are found on the southeast coast of North America and in the northern parts of Eurasia.

9

corr Nov–Mar averaged ssw monthly
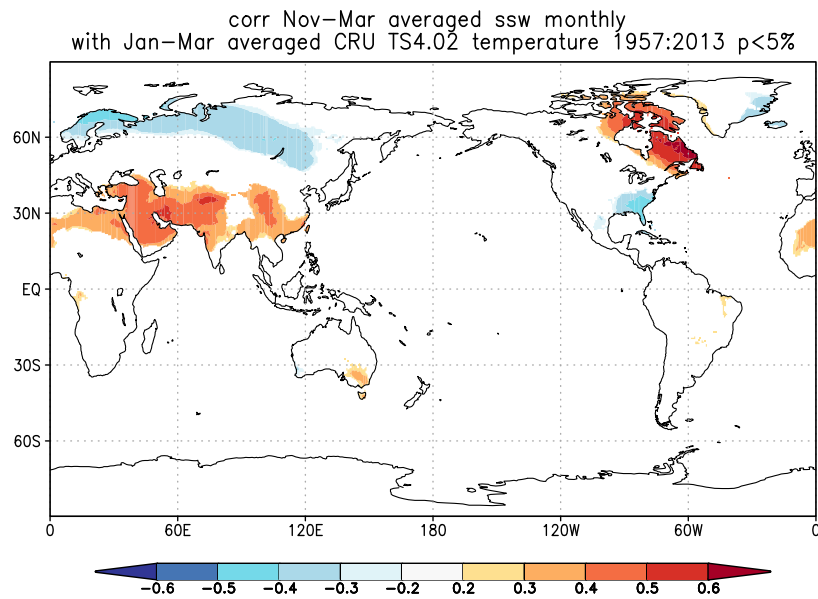with Jan–Mar averaged CRU TS4.02 temperature 1957:2013 p<5%

Figure 5: Spatial correlations between winter average of SSW series and January–March mean surface temperature. Strong correlations are seen in: (positive) northeastern North America and Africa and southern Eurasia, (negative) northern Eurasia.

Correlations between SSWs and average temperature in February–April shown (see Figure 6) strong, positive, correlations in northeastern North America, northeastern Africa and southern Asia. Negative correlations are seen in northern Eurasia. Extent and intensity is increased in Eurasia compared to figure 5.
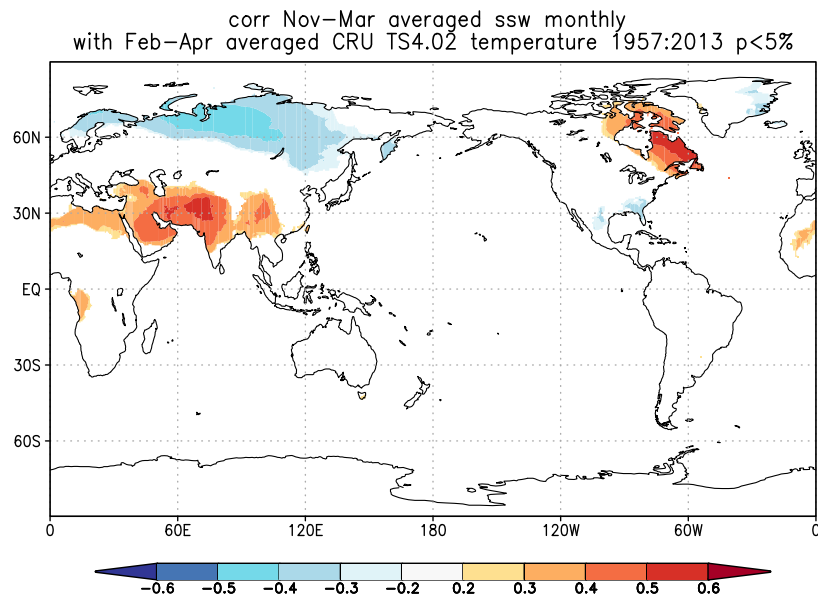
Figure 6: Spatial correlations between winter average of SSW series and February–April mean surface temperature. Strong correlations are seen in: (positive) northeastern North America and southern Asia, (negative) northern Eurasia.

Regions where SSWs are significantly correlated to average January–March temperature anomalies are found (see Figure 7) in northern Eurasia (negative) and central Asia (positive). Hardly any coherent regions of correlation are seen in North America.

corr Nov–Mar averaged ssw monthly
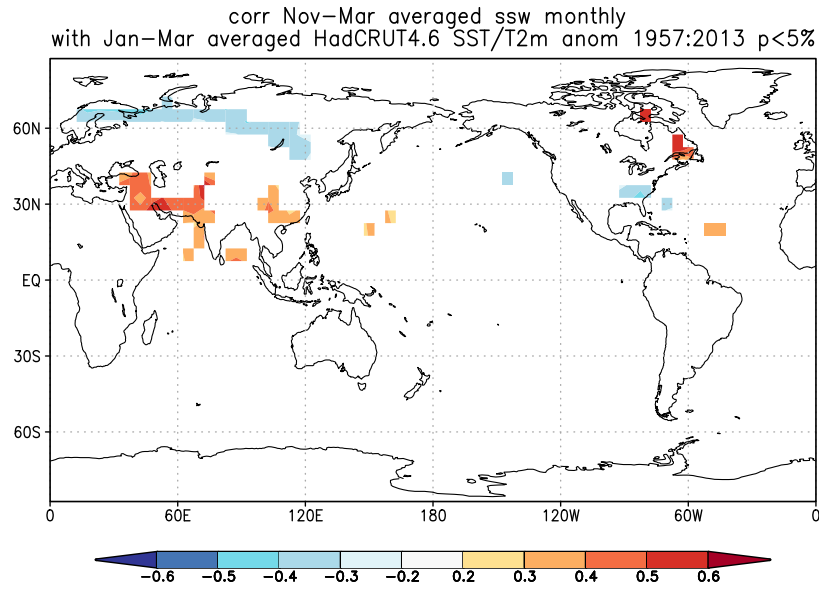with Jan–Mar averaged HadCRUT4.6 SST/T2m anom 1957:2013 p<5%

Figure 7: Spatial correlations between winter average of SSW series and January–March mean surface temperature anomalies. Strong correlations are seen in central Asia (positive) and northern Eurasia (negative).

The percentage of days in the 10th percentile for daily minimum temperature is strongly correlated to the winter average of the SSW series in the northern parts of Scandinavia and Eurasia. A slight positive development of the correlated areas can be seen between the January–March (see Figure 8) and February–April (see Figure 9) averages, the main increases can be seen in northeastern Asia. The negatively correlated areas in northeastern North America, Greenland, northeastern Africa and western Asia are decreasing between the two time periods.
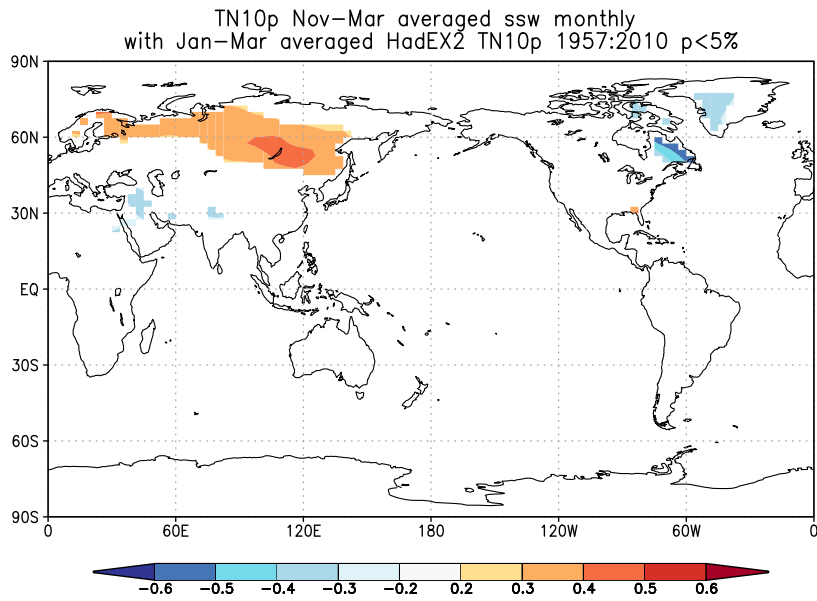
Figure 8: Spatial correlations between the winter average of the SSW series and January–March average percentage of days in the 10th percentile of daily minimum temperature. Strong positive correlations are seen in northern Scandinavia and Eurasia. A weaker, negative, correlation is seen in northeastern North America, Greenland, northeastern Africa and western Asia.
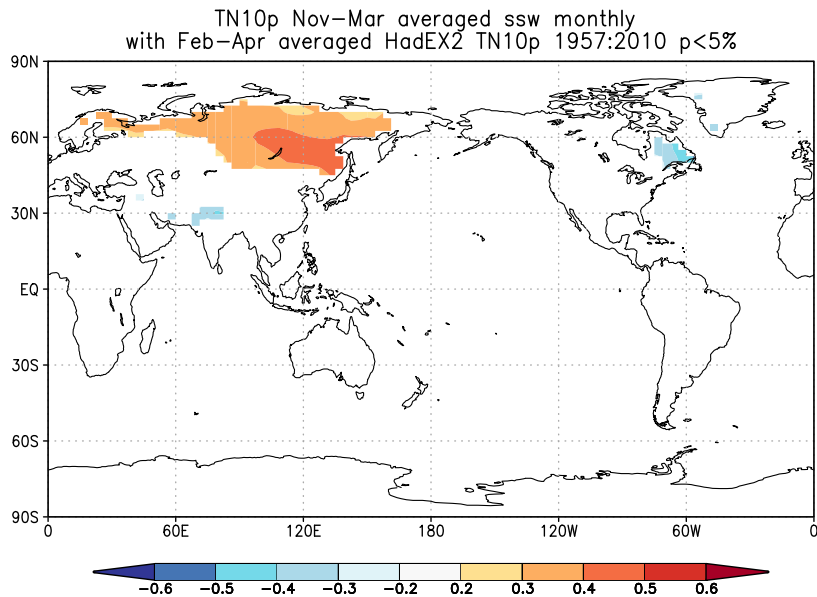

Figure 9: Spatial correlations between winter average of SSW series and February–April average percentage of days in the 10th percentile of daily minimum temperature. Strong positive correlations are seen in the northern parts of Scandinavia and Eurasia. A weaker, negative, correlation is seen in northeastern North America, Greenland and western Asia.

3.3 Regional analysis: Sodankylä and Fort Chimo

Comparing the mean monthly temperature during years with SSW occurring to years when no SSWs occur show (see Figure 10a) a small negative influence on monthly mean temperature during November to April in Sodankylä. The 10th and 90th percentiles are also lower than their non-SSW counter parts, but the span is roughly similar. Monthly mean temperatures in Fort Chimo display (see Figure 10b) an opposite reaction to SSWs compared to Sodankylä. Between December and April a positive increase in mean temperature is displayed during SSW years compared to non-SSW years. The span of the 10th and 90th percentiles is also wider during SSW years than during non-SSW years, particularly due to a higher 10th percentile during SSW years. In both locations no influence on monthly mean temperature is seen from May until October.
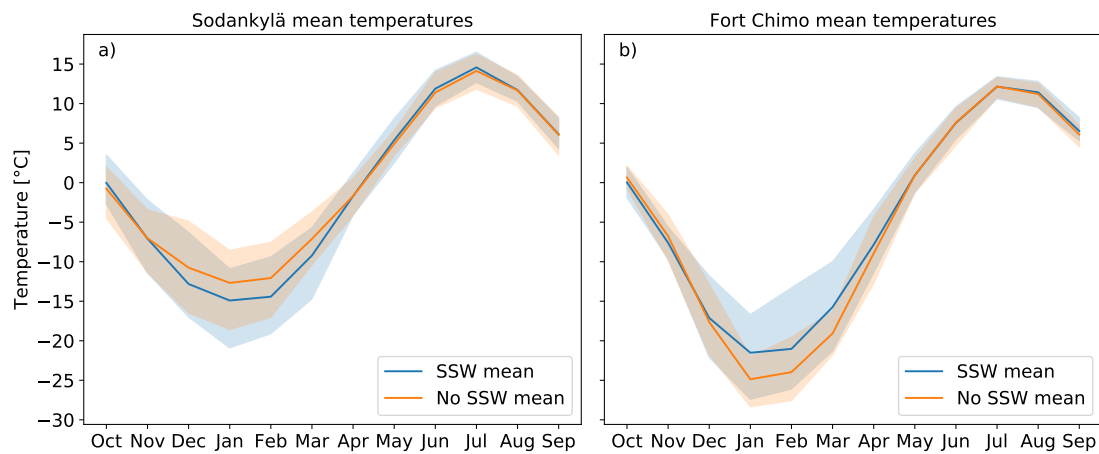

Figure 10: Comparisons between monthly mean temperatures during years with SSWs occurring (blue lines) and years with no SSWs occurring (orange lines) in: a) Sodankylä, Finland, and b) Fort Chimo, Canada. Shaded areas indicate extent of 10th and 90th percentiles. The locations display opposite reactions to SSWs during winter.

Further more, Sodankylä exhibits significant negative correlations during the four periods between December and April (see Figure 11a). The periods are significant at p<0.05. February to March display the strongest correlation: $r \approx -0.38$, $p < 0.05$. The temperatures in Fort Chimo (see Figure 11b) are positively correlated ($p < 0.01$) during the four periods between December and April. For the periods between December and April p<0.01. February to March display the strongest correlation: $r \approx 0.45$, $p < 0.01$.
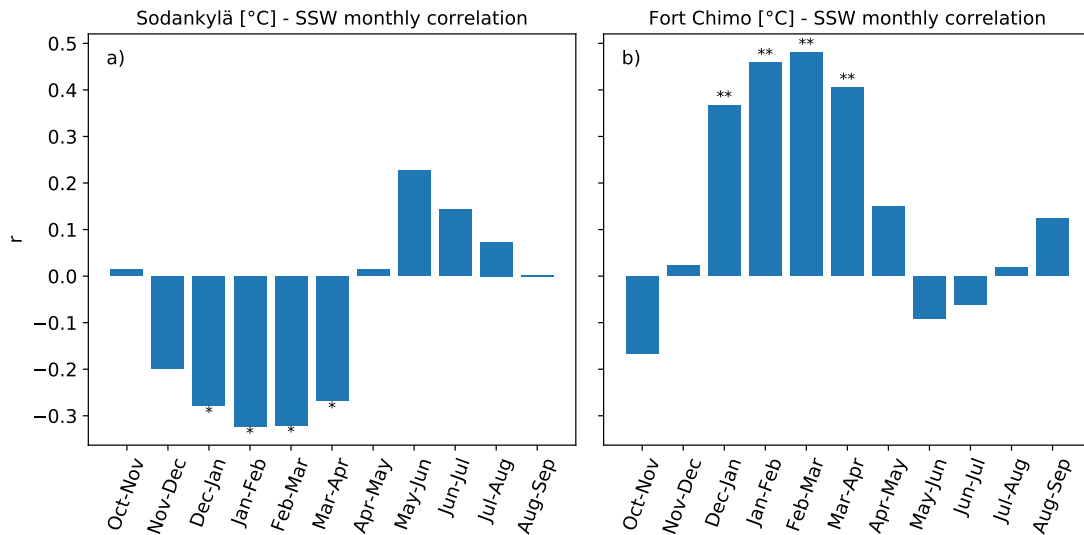
*Figure 11: R-values from correlating the November–March mean SSW value against a two month running mean temperature. Period significance is indicated by *: $p < 0.05$ and **: $p < 0.01$. a) Sodankylä display significant negative correlations between January and April. b) Fort Chimo display significant positive correlations between December and April.*

The temperature series from Sodankylä and Fort Chimo exhibit (see Figure 12) relatively strong anti-correlations ($p < 0.01$) during all the two month mean periods between December and April. R-values are ranging from -0.36 in December–January to -0.54 in February–March. During the summer months no significant relationships are displayed. .
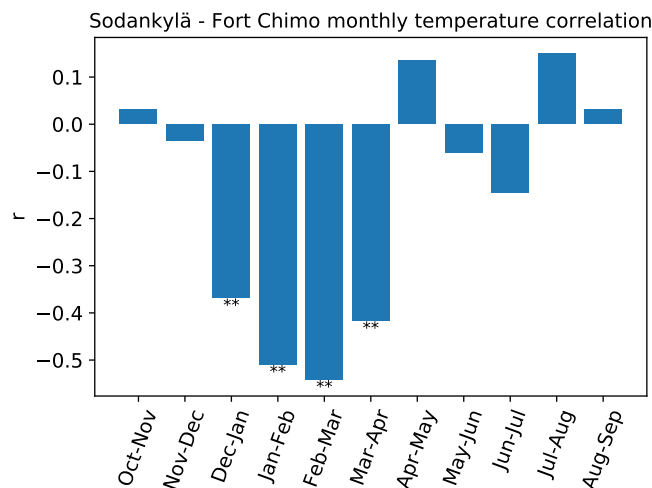
*Figure 12: Resulting r-values from Sodankylä two–month mean temperature correlation against Fort Chimo two–month mean temperature during the years 1958 – 2013. ** indicates period significance at $p < 0.01$. Significant correlations are exhibited during the four periods between December and April.*

January–April mean temperature in Sodankylä exhibit (see Table 4) a negative correlation to the November–March mean SSW value. The December–April mean

temperature in Fort Chimo are positively correlated to the November–March mean SSW value. Sodankylä November–March mean temperature exhibits a negative correlation against the Fort Chimo November–March mean temperature.

Table 4: Results from the selected period mean correlations. SK: Sodankylä. FC: Fort Chimo.

Variables	r	p
SK Jan–Apr mean Tmp. & Nov–Mar mean SSW	-0.38	0.004
FC Dec–Apr mean Tmp. & Nov–Mar mean SSW	0.53	$2.5 \cdot 10^{-5}$
SK Nov–Mar mean Tmp. & FC Nov–Mar mean Tmp.	-0.44	$6.5 \cdot 10^{-4}$

4   Discussion

4.1   The connection between SSWs, AO, NAO and temperature

Investigating the relationship between an SSW event and the AO revealed a moderate connection during the winter months. The analysis (see Figure 3a) suggests a weak but significant correlation between SSW events and the AO during the two month periods between January and April. The NAO exhibits a slightly weaker connection to SSWs, significant correlation are present in the three periods between January and March. None of the indices display any significant correlations in the early winter months. This is most likely a result of the low number of SSWs (see Table 3) occurring during these periods, two and five in November and December, hence no significant connection can be established. That the correlation increases during mid winter months could be explained by the increased number of events that occur during this period. A more fundamental interpretation can be the formation of the polar vortex, which usually forms in the early winter months. The mean zonal westerlies of the polar vortex allows planetary waves to propagate upward from the troposphere, resulting in larger amplitudes in the AO (Baldwin, Cheng, & Dunkerton, 1994; Baldwin & Dunkerton, 1999). This also aligns well with the absence of any significant correlations during the summer months since there is no polar vortex forcing the AO and NAO.

Perlwitz and Graf (1995) and Wang and Chen (2010) both show that the strength of the polar vortex is affecting the geopotential heights at the tropospheric level (850 hPa) in regions associated with the AO and thus has a analogous relationship with the strength of the AO. Because of this it can be expected that years with SSWs, i.e. weak polar vortex events, display a higher frequency of negative AO index values than the years when no such events occur. This is what is displayed in figure 4a and further confirmed by the significantly ($p<0.05$) lower than zero winter mean AO index during SSWs years. The non-SSW mean winter AO index is not distinguishable from zero (see Figure 4a), hence no bias is detected towards either positive or negative values during non-SSW years.

Ambaum et al. (2001) concluded that due to the larger loading pattern of the AO compared to for example NAO, a different set of physical properties might

be involved in the variability of the AO, and that this larger loading pattern might dilute a possible signal of stratospheric anomalies. Interestingly enough they suggest that a division of AO into NAO and PNA (Pacific/North American pattern) could provide more information about the physical state of the Northern Hemisphere. However, results in this thesis suggest AO as a, although only slightly, better candidate concerning a signal of SSWs in the troposphere based on the stronger correlations and distribution patterns presented in figure 3 and 4. This is more in line with the findings from Thompson and Wallace (2000).

The spatial correlations regarding precipitation did not yield any maps with a p-field value <0.1, hence no connections between SSWs and precipitation can be considered based on the extent of this analysis. Temperature on the other hand display multiple regions with moderate correlations to SSWs. The three main areas displaying a positive correlation to SSWs are the northeastern part of North America, the southern parts of central Asia and northeastern parts of Africa. An area encompassing the northern parts of Eurasia display a negative correlation to SSWs. All the areas display (see Figure 5 and 6) a slight increase in the intensity and extent of the correlated fields of the January–March mean compared to the February–April mean.

Findings from Hitchcock and Simpson (2014) show patterns very similar to these results both in the locations and proposed sign of the correlations from this study. What makes it even more interesting is that this study is based on observational data while Hitchcock and Simpson based their study on modelled data. Findings in this study however does not exhibit the large negatively affected areas in interior North America and Europe that Hitchcock and Simpson found. This disparity in the results could be contributed to the distinction between calculating a difference between two models run on different inputs (as done by Hitchcock and Simpson) and correlating two sets of observational data, only keeping the significant results (as done in this study).

The patterns that can be seen in the anomaly field correlation maps (see Figure 7) are not as distinct as those in the temperature data. This could be an artefact of the lower resolution of the data set (see Table 2) compared to the resolution of the temperature data. No anomaly data was available at same resolution as the CRU TS 4.01 data set. This could also be the reason why no coherent regions of correlations are displayed in northeastern North America. Correlations between SSWs and temperature anomalies is of interest since it provides proof that SSWs forces temperatures to deviate from the climatological mean more than the natural variation.

This is further confirmed by the significant correlations that the SSWs exhibit against the percentage of days with temperatures within the 10th percentile of the daily minimum temperature of that month. This can be compared to the increased probability of unusually cold winter months in connection to SSWs presented by Kolstad et al. (2010). Spatial patterns in the 10th percentile temperature correlations (see Figure 8 and 9) are also very similar to the mean temperature correlations (see Figure 5,6 and 7), further strengthening that these are the areas of interest investigating the regional effects of SSWs.

4.2   Regional analysis: Sodankylä and Fort Chimo

Sodankylä and Fort Chimo were chosen based on their location within the areas of interest and the complete time coverage of the SSW time series. Sodankylä exhibits a negative trend in mean monthly temperatures during SSW winters, between November and March a decrease of $\sim 3°$C can be observed in figure 10a. The decrease in the 10th and 90th percentiles is on a similar magnitude, never being more than a few degrees lower than the non-SSW years. Since it is close to the natural variations it would be difficult to distinguish a SSW year from a non-SSW year on the mean temperature data. During the winter months in Fort Chimo the mean monthly temperature instead increases during a SSW year. It even approaches the 90th percentile level of the non-SSW year in January and March (see Figure 10b). Based on this, and because of the increased variation seen in the extent of the 90th percentile during the same period, SSW winters can be considered unusually warm in Fort Chimo.

The lack of distinction between the SSW and non-SSW means, 10th and 90th percentiles during May until October (see Figure 10a and 10b) indicate that there is no temperature signal from SSWs extending into these months, further confirmed by the lack of significant correlations (see Figure 11) during the same period.

Investigating the relationship between Sodankylä and Fort Chimo further revealed (see Figure 12) a significant negative correlation between the mean winter temperatures of the two locations, both for the two month running means and the whole winter period. The same inverse pattern is present in the spatial correlation maps (see Figure 5 and 6). This inverse relationship between the two locations, regardless of the occurrence of SSWs or not, indicates the possibility of a teleconnection concerning temperature between the two locations. Van Loon and Rogers (1978) found that the opposing variation between the Icelandic low pressure and the Azores high and Aleutian low pressures, and the resulting inverse relationship between the Pacific and Atlantic westerlies, could suggest a connection between the North Atlantic and Pacific oscillations. This would be responsible for the so called winter temperature seesaw between northeastern North America and northern Europe. Findings from Thompson et al. (2002), Hurrell (1995) and Kidston et al. (2015) suggest that the majority of North America also exhibits a negative response in temperature to SSWs similar to northern Eurasia and that the positive response in the northeastern area is a signature of the NAO.

To completely establish the relationship between SSWs and the AO, NAO and surface temperature the next step would be to try and classify known SSW years based on analysis of AO, NAO and temperature data from northeastern Canada. This vital link is needed if SSW occurrences are to be reconstructed from proxy data.

4.3   The possibility of a SSW signal in climate reconstructions

Using proxy data for climate variability such as tree ring width and ice accumulation the summer season AO and NAO (Appenzeller, Stocker, & Anklin, 1998;

Cook, Arrigo, & Briffa, 1998; Luterbacher et al., 2001; D'Arrigo, Cook, Mann, & Jacoby, 2003; Ortega et al., 2015) and the winter season NAO (Cook, D'Arrigo, & Mann, 2002) has been reconstructed successfully. Since the highest possible temporal resolution from climate proxies is interannual it requires the signal of SSWs to have a clear effect on seasonal values of the climate variable. Findings of this study point to a significant difference in the mean winter AO index during SSW years compared to non-SSW years, however SSWs are not the main driver behind the variability of the AO and NAO (Fyfe et al., 1999). Hence a winter exhibiting a unusually low AO index can not be considered an indication of the occurrence of a SSW alone.

Mean monthly temperature display a signal of SSWs in Fort Chimo during the winter months, both at the bi-monthly time scale and during the whole winter season (see Figure 10b and Table 4). Reconstructions of temperature based on tree ring data are usually done on spring and summer temperatures (Jacoby & D'Arrigo, 1989; Briffa et al., 1990). However, some studies suggests a possible winter sensitivity. Zhu, Fang, Shao, and Yin (2009) reconstructed the February–April temperature in the Changbai Mountains in northeastern China based on tree ring widths from Korean pines. This is based on the assumption that pre growth season climatic conditions can influence the radial growth of trees via either direct impacts damaging the root systems and foliage of the tree or an indirect effect such as delayed snow melts (Peterson & Peterson, 2001; Pederson, Cook, Jacoby, Peteet, & Griffin, 2004). Date of snow melt is a result of winter precipitation and early summer temperature and will determine the initiation of cambium activity, hence affecting tree growth throughout the season (Kirdyanov, Hughes, Vaganov, Schweingruber, & Silkin, 2003).

Gennaretti, Arseneault, Nicault, Perreault, and Bégin (2014) gathered tree rings from the northeastern North America to investigate the possibility of a volcano-induced regime shift in millennial trees. This was done through the reconstruction of summer temperature based on sub-fossil black spruce (*Picea mariana*) from the northeastern North American taiga. Although SSWs don't exhibit any signals in summer temperatures in northeastern Canada, tree data from this research could be a good candidate for the investigation of a SSWs signal in tree rings. Trees in this area will be growing at their northern range margin, which according to Pederson et al. (2004) could make them sensitive to winter temperatures, and thus enabling the possibility of SSW signal.

Due to the limited time frame of this thesis a thorough analysis of tree data was not possible. For the sake of discussion and as encouragement to future research a simple comparison between the yearly SSW series and tree ring data from the Gennaretti et al. Lake L1 Quebec site was done. A total of 17 trees covered the time period 1958–2011. Raw ring width measurements from tree L1V14 showed (see Figure 13) the highest correlation against the SSW time series.
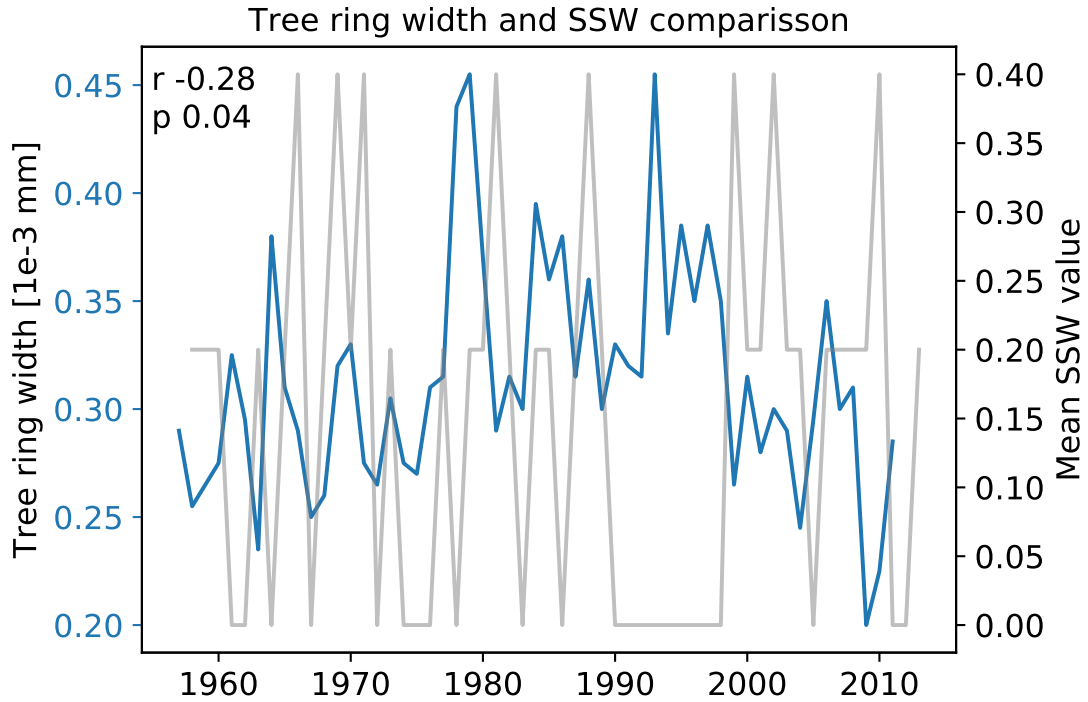
Figure 13: Raw ring width measurements from tree L1V14 in the Lake L1 Quebec site (blue) compared to the yearly SSW time series (grey). The two time series exhibit a significant negative correlation.

Interestingly enough this particular tree display a negative correlation against the SSW time series. Since the SSW series has shown a positive effect on winter temperatures in the northeastern North America area (see Figure 10, 5 6) it could be theorised that a positive correlation could exist between SSWs and tree ring width. However, since mean temperatures never reach levels close to growth initiation, a direct relation is not likely. Instead an indirect effect such as delayed snow melts should be considered. It is worth noting that this data is not de-trended in any way, hence any climatic signal might be lost in the natural growth trends of the tree. A winter temperature reconstruction based on trees in this area would be good next step in the pursuit of a SSW reconstruction.

4.4 Limits to method

A large part of the analysis rely on statistical methods to identify the relationship between different climatical parameters. To completely rely on statistics establishing physical relationships is not considered good practice, hence tests performed in this study are done to investigate the strength of relationships already established in the scientific field. Between the SSW time series and the different climatic variables *Spearman's* correlation was performed. This was done because of the non-parametric nature of the SSW data and that it's not normally distributed, two conditions that *Pearson's* correlation requires. According to this, associations between the climatic variables was checked with *Pearson's* correlation.

5   Conclusion

The aim of this thesis was to investigate the possibility of a signal of SSWs in surface climate. Both the AO and NAO exhibits a signal of SSWs in their respective November–March means, with AO displaying a slightly stronger signal. However, only a small part of the variance within the AO and NAO can be explained by the occurrences of SSWs. Because of this neither the AO or the NAO are considered suitable climatic variables for identifying a clear signal of SSWs single-handedly.

Spatial correlations performed on the November–March mean SSW value against the three month running mean temperature and precipitation revealed a relatively strong positive connection between temperature and SSWs in northeastern North America and Africa and southern Asia. Negative connections are found in northern Eurasia. No regions exhibited any connections between precipitation and SSWs.

A more detailed study of Sodankylä (northern Finland) and Fort Chimo (northeastern Canada) further strengthened the inverse temperature relationship displayed in the spatial correlation. Mean winter temperatures in Sodankylä during SSW years are only slightly lower than during non-SSW years. In Fort Chimo the mean winter temperatures during SSW years exceeds the 90th percentile of the winter temperature during non-SSW years during January and March. None of the locations show any changes in mean temperature due to SSWs between April and October. Investigating the possibility of detecting known SSW years based on winter means of AO, NAO and temperatures in northeastern North America is suggested as the next step to establish the link between SSWs and surface climate.

Since mean temperatures at neither of the locations reach into levels that could be considered as favourable growth conditions during SSW winters no direct effects on tree growth are considered as a reason why trees would exhibit a signal of SSWs. Instead indirect effects such as delayed snow melt or root damage are considered as possible causes of sensitivity to winter temperatures that can be affected by SSWs.

In the continued investigation of climate proxies for SSWs, tree rings from northeastern North America are suggested as good candidates for proxy data for two reasons:

1. The region exhibit a strong connection between higher mean winter temperatures and the occurrence of SSWs.

2. Trees in this region will grow at their northern margin, possibly making them more sensitive to winter temperatures.

A winter temperature reconstruction based on the data from e.g. Gennaretti et al. (2014) could be used in the potential detection of SSWs in paleoclimatic data.

6   Acknowledgements

References

Ambaum, M. H. P., Hoskins, B. J., Stephenson, D. B., Ambaum, M. H. P., Hoskins, B. J., & Stephenson, D. B. (2001, 8). Arctic Oscillation or North Atlantic Oscillation? *Journal of Climate*, *14*(16), 3495–3507. Retrieved from http://journals.ametsoc.org/doi/abs/10.1175/1520-0442%282001%29014%3C3495%3AAOONAO%3E2.0.CO%3B2

Appenzeller, C., Stocker, T. F., & Anklin, M. (1998, 10). North atlantic oscillation dynamics recorded in greenland ice cores. *Science (New York, N.Y.)*, *282*(5388), 446–9. Retrieved from http://www.ncbi.nlm.nih.gov/pubmed/9774265

Baldwin, M. P., Cheng, X., & Dunkerton, T. J. (1994). Observed correlations between winter-mean tropospheric and stratospheric circulation anomalies. *Geophysical Research Letters*, *21*(12), 1141–1144. Retrieved from https://agupubs.onlinelibrary.wiley.com/doi/pdf/10.1029/94GL01010

Baldwin, M. P., & Dunkerton, T. J. (1999, 12). Propagation of the Arctic Oscillation from the stratosphere to the troposphere. *Journal of Geophysical Research Atmospheres*, *104*(D24), 30937–30946. Retrieved from http://doi.wiley.com/10.1029/1999JD900445

Baldwin, M. P., & Dunkerton, T. J. (2001, 10). Stratospheric harbingers of anomalous weather regimes. *Science (New York, N.Y.)*, *294*(5542), 581–4. Retrieved from http://www.ncbi.nlm.nih.gov/pubmed/11641495

Bradley, R. S. (1999). *Paleoclimatology: reconstructing climates of the Quaternary.* Elsevier.

Briffa, K. R. (2000, 1). Annual climate variability in the Holocene: interpreting the message of ancient trees. *Quaternary Science Reviews*, *19*(1-5), 87–105. Retrieved from https://www.sciencedirect.com/science/article/pii/S0277379199000566

Briffa, K. R., Bartholin, T. S., Eckstein, D., Jones, P. D., Karlén, W., Schweingruber, F. H., & Zetterberg, P. (1990, 8). A 1,400-year tree-ring record of summer temperatures in Fennoscandia. *Nature*, *346*(6283), 434–439. Retrieved from http://www.nature.com/articles/346434a0

Butler, A. H., Seidel, D. J., Hardiman, S. C., Butchart, N., Birner, T., Match, A., . . . Match, A. (2015, 11). Defining Sudden Stratospheric Warmings. *Bulletin of the American Meteorological Society*, *96*(11), 1913–1928. Retrieved from http://journals.ametsoc.org/doi/10.1175/BAMS-D-13-00173.1

Butler, A. H., Sjoberg, J. P., Seidel, D. J., & Rosenlof, K. H. (2017, 2). A sudden stratospheric warming compendium. *Earth System Science Data*, *9*(1), 63–76. Retrieved from https://www.earth-syst-sci-data.net/9/63/2017/

Compo, G. P., Whitaker, J. S., Sardeshmukh, P. D., Matsui, N., Allan, R. J., Yin, X., . . . Worley, S. J. (2011, 1). The Twentieth Century Reanalysis Project. *Quarterly Journal of the Royal Meteorological Society*, *137*(654), 1–28. Retrieved from http://doi.wiley.com/10.1002/qj.776

Cook, E. R., Arrigo, R. D., & Briffa, K. R. (1998). The North Atlantic Oscillation and its expression in circum-Atlantic tree-ring chronolgies from North America and Europe. *The Holocene*, *8*, 9–17. Retrieved from `https://journals.sagepub.com/doi/pdf/10.1191/095968398677793725`

Cook, E. R., D'Arrigo, R. D., & Mann, M. E. (2002). A well-verified, multiproxy reconstruction of the winter North Atlantic Oscillation index since A.D. 1400. *Journal of Climate*, *15*(13), 1754–1764. Retrieved from `https://journals.ametsoc.org/doi/pdf/10.1175/1520-0442(2002)015%3C1754%3AAWVMRO%3E2.0.CO%3B2`

D'Arrigo, R. D., Cook, E. R., Mann, M. E., & Jacoby, G. C. (2003, 6). Tree-ring reconstructions of temperature and sea-level pressure variability associated with the warm-season Arctic Oscillation since AD 1650. *Geophysical Research Letters*, *30*(11), 1549. Retrieved from `http://doi.wiley.com/10.1029/2003GL017250`

Dee, D. P., Uppala, S. M., Simmons, A. J., Berrisford, P., Poli, P., Kobayashi, S., ... Vitart, F. (2011, 4). The ERA-Interim reanalysis: configuration and performance of the data assimilation system. *Quarterly Journal of the Royal Meteorological Society*, *137*(656), 553–597. Retrieved from `http://doi.wiley.com/10.1002/qj.828`

Donat, M. G., Alexander, L. V., Yang, H., Durre, I., Vose, R., Dunn, R. J. H., ... Kitching, S. (2013, 3). Updated analyses of temperature and precipitation extreme indices since the beginning of the twentieth century: The HadEX2 dataset. *Journal of Geophysical Research: Atmospheres*, *118*(5), 2098–2118. Retrieved from `http://doi.wiley.com/10.1002/jgrd.50150`

Fyfe, J. C., Boer, G. J., & Flato, G. M. (1999, 6). The Arctic and Antarctic oscillations and their projected changes under global warming. *Geophysical Research Letters*, *26*(11), 1601–1604. Retrieved from `http://doi.wiley.com/10.1029/1999GL900317`

Garfinkel, C. I., Feldstein, S. B., Waugh, D. W., Yoo, C., & Lee, S. (2012, 9). Observed connection between stratospheric sudden warmings and the Madden-Julian Oscillation. *Geophysical Research Letters*, *39*(18). Retrieved from `http://doi.wiley.com/10.1029/2012GL053144`

Gennaretti, F., Arseneault, D., Nicault, A., Perreault, L., & Bégin, Y. (2014, 7). Volcano-induced regime shifts in millennial tree-ring chronologies from northeastern North America. *Proceedings of the National Academy of Sciences of the United States of America*, *111*(28), 10077–82. Retrieved from `http://www.ncbi.nlm.nih.gov/pubmed/24982132http://www.pubmedcentral.nih.gov/articlerender.fcgi?artid=PMC4104845`

Harris, I., Jones, P., Osborn, T., & Lister, D. (2014, 3). Updated high-resolution grids of monthly climatic observations - the CRU TS3.10 Dataset. *International Journal of Climatology*, *34*(3), 623–642. Retrieved from `http://doi.wiley.com/10.1002/joc.3711`

Hitchcock, P., & Simpson, I. R. (2014, 10). The Downward Influence of

Stratospheric Sudden Warmings. *Journal of the Atmospheric Sciences*, *71*(10), 3856–3876. Retrieved from `http://journals.ametsoc.org/doi/abs/10.1175/JAS-D-14-0012.1`

Holton, J. R., & Tan, H.-C. (1980, 10). The Influence of the Equatorial Quasi-Biennial Oscillation on the Global Circulation at 50 mb. *Journal of the Atmospheric Sciences*, *37*(10), 2200–2208. Retrieved from `http://journals.ametsoc.org/doi/abs/10.1175/1520-0469%281980%29037%3C2200%3ATIOTEQ%3E2.0.CO%3B2`

Hurrell, J. W. (1995, 8). Decadal trends in the north atlantic oscillation: regional temperatures and precipitation. *Science (New York, N.Y.)*, *269*(5224), 676–9. Retrieved from `http://www.ncbi.nlm.nih.gov/pubmed/17758812`

Jacoby, G. C., & D'Arrigo, R. (1989, 2). Reconstructed Northern Hemisphere annual temperature since 1671 based on high-latitude tree-ring data from North America. *Climatic Change*, *14*(1), 39–59. Retrieved from `http://link.springer.com/10.1007/BF00140174`

Kalnay, E., Kanamitsu, M., Kistler, R., Collins, W., Deaven, D., Gandin, L., … Joseph, D. (1996, 3). The NCEP/NCAR 40-Year Reanalysis Project. *Bulletin of the American Meteorological Society*, *77*(3), 437–471. Retrieved from `http://journals.ametsoc.org/doi/abs/10.1175/1520-0477%281996%29077%3C0437%3ATNYRP%3E2.0.CO%3B2`

Kang, W., Tziperman, E., Kang, W., & Tziperman, E. (2017, 11). More Frequent Sudden Stratospheric Warming Events due to Enhanced MJO Forcing Expected in a Warmer Climate. *Journal of Climate*, *30*(21), 8727–8743. Retrieved from `http://journals.ametsoc.org/doi/10.1175/JCLI-D-17-0044.1`

Kidston, J., Scaife, A. A., Hardiman, S. C., Mitchell, D. M., Butchart, N., Baldwin, M. P., & Gray, L. J. (2015, 6). Stratospheric influence on tropospheric jet streams, storm tracks and surface weather. *Nature Geoscience*, *8*(6), 433–440. Retrieved from `http://www.nature.com/articles/ngeo2424`

Kirdyanov, A., Hughes, M., Vaganov, E., Schweingruber, F., & Silkin, P. (2003, 1). The importance of early summer temperature and date of snow melt for tree growth in the Siberian Subarctic. *Trees*, *17*(1), 61–69. Retrieved from `http://link.springer.com/10.1007/s00468-002-0209-z`

KNMI. (2019). *Climate Explorer.* Retrieved from `https://climexp.knmi.nl/`

Kobayashi, S., Ota, Y., Harada, Y., Ebita, A., Moriya, M., Onoda, H., & ... & Miyaoka, K. (2015). The JRA-55 reanalysis: General specifications and basic characteristics. *Journal of the Meteorological Society of Japan. Ser. II*, *93*(1), 5–48. Retrieved from `https://www.jstage.jst.go.jp/article/jmsj/93/1/93_2015-001/_article/-char/ja/`

Kolstad, E. W., Breiteig, T., & Scaife, A. A. (2010, 5). The association between stratospheric weak polar vortex events and cold air outbreaks in the Northern Hemisphere. *Quarterly Journal of the Royal Meteorological Society*, *136*(649), 886–893. Retrieved from `http://doi.wiley.com/10.1002/qj.620`

Limpasuvan, V., Thompson, D. W. J., & Hartmann, D. L. (2004). The Life Cycle of the Northern Hemisphere Sudden Stratospheric Warmings. *Journal of Climate*, *17*(13), 2584–2596. Retrieved from `https://journals.ametsoc.org/doi/pdf/10.1175/1520-0442(2004)017%3C2584%3ATLCOTN%3E2.0.CO%3B2`

Luterbacher, J., Xoplaki, E., Dietrich, D., Jones, P. D., Davies, T. D., Portis, D., . . . Wanner, H. (2001). Extending North Atlantic Oscillation reconstructions back to 1500. *Atmospheric Science Letters*, *2*(1-4), 114–124. Retrieved from `http://dss.ucar.edu/datasets/ds010.1/data/`

Marshak, S. (2015). *Earth: Portrait of a Planet: 5th International Student Edition* (5th ed.). London: WW Norton & Company.

Mayewski, P. A., Rohling, E. E., Curt Stager, J., Karlén, W. W., Maasch, K. A., Meeker, L. D., . . . Steig, E. J. (2004, 11). Holocene climate variability. *Quaternary Research*, *62*(3), 243–255. Retrieved from `www.elsevier.com/locate/yqreshttps://www.cambridge.org/core/product/identifier/S0033589400026892/type/journal_article`

Mercer, J. B. (2003, 5). Cold—an underrated risk factor for health. *Environmental Research*, *92*(1), 8–13. Retrieved from `https://www.sciencedirect.com/science/article/pii/S0013935102000099`

Molod, A., Takacs, L., Suarez, M., & Bacmeister, J. (2015). Development of the GEOS-5 atmospheric general circulation model: evolution from MERRA to MERRA2. *Geosci. Model Dev*, *8*, 1339–1356. Retrieved from `www.geosci-model-dev.net/8/1339/2015/`

Morice, C. P., Kennedy, J. J., Rayner, N. A., & Jones, P. D. (n.d.). *Quantifying uncertainties in global and regional temperature change using an ensemble of observational estimates: the HadCRUT4 data set* (Tech. Rep.). Retrieved from `https://www.metoffice.gov.uk/hadobs/hadcrut4/HadCRUT4_accepted.pdf`

Nash, E. R., Newman, P. A., Rosenfield, J. E., & Schoeberl, M. R. (1996). *An objective determination of the polar vortex using Ertel's potential vorticity* (Vol. 101; Tech. Rep. No. D5). Retrieved from `https://agupubs.onlinelibrary.wiley.com/doi/pdf/10.1029/96JD00066`

NOAA. (n.d.-a). *Arctic Oscillation (AO) | Teleconnections | National Centers for Environmental Information (NCEI).* Retrieved from `https://www.ncdc.noaa.gov/teleconnections/ao/`

NOAA. (n.d.-b). *North Atlantic Oscillation (NAO) | Teleconnections | National Centers for Environmental Information (NCEI).* Retrieved from `https://www.ncdc.noaa.gov/teleconnections/nao/`

Ortega, P., Lehner, F., Swingedouw, D., Masson-Delmotte, V., Raible, C. C., Casado, M., & Yiou, P. (2015). A model-tested North Atlantic Oscillation reconstruction for the past millennium. *Nature*, *523*(7558), 71–74. Retrieved from `http://climatehomes.unibe.ch/~lehner/papers/ortega15nat.pdf`

Pachauri, R. K., Allen, M. R., Barros, V. R., Broome, J., Cramer, W., Christ, R., . . . others (2014). *Climate change 2014: synthesis report. Contribution of Working*

Groups I, II and III to the fifth assessment report of the Intergovernmental Panel on Climate Change. Ipcc.

Pederson, N., Cook, E. R., Jacoby, G. C., Peteet, D. M., & Griffin, K. L. (2004, 12). The influence of winter temperatures on the annual radial growth of six northern range margin tree species. *Dendrochronologia*, *22*(1), 7–29. Retrieved from `https://www.sciencedirect.com/science/article/pii/S1125786504000128`

Perlwitz, J., & Graf, H.-F. (1995, 10). The Statistical Connection between Tropospheric and Stratospheric Circulation of the Northern Hemisphere in Winter. *Journal of Climate*, *8*(10), 2281–2295. Retrieved from `http://journals.ametsoc.org/doi/abs/10.1175/1520-0442%281995%29008%3C2281%3ATSCBTA%3E2.0.CO%3B2`

Peterson, D. W., & Peterson, D. L. (2001, 12). Mountain hemlock growth responds to climatic variability at annual and decadal time scales. *Ecology*, *82*(12), 3330–3345. Retrieved from `https://esajournals.onlinelibrary.wiley.com/doi/abs/10.1890/0012-9658(2001)082%5B3330:MHGRTC%5D2.0.CO%3B2`

Pinto, J. G., Brücher, T., Fink, A. H., & Krüger, A. (2007, 1). Extraordinary snow accumulations over parts of central Europe during the winter of 2005/06 and weather-related hazards. *Weather*, *62*(1), 16–21. Retrieved from `http://doi.wiley.com/10.1002/wea.19`

Schimanke, S., Spangehl, T., Huebener, H., & Cubasch, U. (2013, 4). Variability and trends of major stratospheric warmings in simulations under constant and increasing GHG concentrations. *Climate Dynamics*, *40*(7-8), 1733–1747. Retrieved from `http://link.springer.com/10.1007/s00382-012-1530-x`

Schoeberl, M. R., & Hartmann, D. L. (1991, 1). The dynamics of the stratospheric polar vortex and its relation to springtime ozone depletions. *Science*, *251*(4989), 46–52.

Schoeberl, M. R., Lait, L. R., Newman, P. A., & Rosenfield, J. E. (1992, 5). The structure of the polar vortex. *Journal of Geophysical Research*, *97*(D8), 7859. Retrieved from `http://doi.wiley.com/10.1029/91JD02168`

Schweingruber, F. H. (1988). *Tree rings: Basics and applications of dendrochronology* (1st ed.). Dordrecht: Kluwer Academic Publishers.

Stohl, A., Bonasoni, P., Cristofanelli, P., Collins, W., Feichter, J., Frank, A., . . . Zerefos, C. (2003, 6). Stratosphere-troposphere exchange: A review, and what we have learned from STACCATO. *Journal of Geophysical Research: Atmospheres*, *108*(D12). Retrieved from `https://agupubs.onlinelibrary.wiley.com/doi/full/10.1029/2002JD002490%4010.1002/%28ISSN%292169-8996.STACCATO1`

The Climate Prediciton Center. (n.d.-a). *Monthly mean AO index since January 1950.* Retrieved from `https://www.cpc.ncep.noaa.gov/products/precip/CWlink/daily_ao_index/ao.shtml`

The Climate Prediciton Center. (n.d.-b). *Monthly mean NAO index since January 1950.* Retrieved from `https://www.cpc.ncep.noaa.gov/products/`

`precip/CWlink/pna/nao.shtml`

Thompson, D. W. J., Baldwin, M. P., & Wallace, J. M. (2002). Stratospheric Connection to Northern Hemisphere Wintertime Weather: Implications for Prediction. *Journal of Climate*, *15*(12), 1421–1428. Retrieved from `https://journals.ametsoc.org/doi/pdf/10.1175/1520-0442(2002)015%3C1421%3ASCTNHW%3E2.0.CO%3B2`

Thompson, D. W. J., & Wallace, J. M. (2000). Annular Modes in the Extratropical Circulation. Part I: Month-to-Month Variability. *Journal of Climate*, *13*(5), 1000–1016. Retrieved from `https://journals.ametsoc.org/doi/pdf/10.1175/1520-0442(2000)013%3C1000%3AAMITEC%3E2.0.CO%3B2`

Uppala, S. M., Allberg, P. W. K., Simmons, A. J., Andrae, U., Da, V., Bechtold, C., ... Woollen, J. (2005). The ERA-40 re-analysis. *Meteorol. Soc*, *131*, 2961–3012. Retrieved from `https://rmets.onlinelibrary.wiley.com/doi/pdf/10.1256/qj.04.176`

Van Loon, H., & Rogers, J. C. (1978, 3). The Seesaw in Winter Temperatures between Greenland and Northern Europe. Part I: General Description. *Monthly Weather Review*, *106*(3), 296–310. Retrieved from `http://journals.ametsoc.org/doi/abs/10.1175/1520-0493%281978%29106%3C0296%3ATSIWTB%3E2.0.CO%3B2`

Wang, L., & Chen, W. (2010, 5). Downward Arctic Oscillation signal associated with moderate weak stratospheric polar vortex and the cold December 2009. *Geophysical Research Letters*, *37*(9). Retrieved from `https://agupubs.onlinelibrary.wiley.com/doi/full/10.1029/2010GL042659%4010.1002/%28ISSN%291944-8007.ATMOSLINKAGES1`

Zhang, C. (2005, 6). Madden-Julian Oscillation. *Reviews of Geophysics*, *43*(2), RG2003. Retrieved from `http://doi.wiley.com/10.1029/2004RG000158`

Zhu, H. F., Fang, X. Q., Shao, X. M., & Yin, Z. Y. (2009). Climate of the Past Tree ring-based February-April temperature reconstruction for Changbai Mountain in Northeast China and its implication for East Asian winter monsoon. *Climate of the Past*, *5*(4), 661–666. Retrieved from `www.clim-past.net/5/661/2009/`

Appendices

A   All SSW events

Table 5: *All the dates of major SSWs found by Butler et al. (2017) when analysing the winds at 60°N and 10hPa in the reanalysis products NCEP-NCAR, ERA40, ERA-Interim, JRA-55 and MERRA2. Empty cells indicate that no data are available. **** indicates that no SSW was detected.*

Event Name	NCEP-NCAR	ERA40	ERA-Interim	JRA-55	MERRA2
JAN 1958	30-Jan-58	31-Jan-58		30-Jan-58	
NOV 1958	30-Nov-58	****		****	
JAN 1960	16-Jan-60	17-Jan-60		17-Jan-60	
JAN 1963	****	28-Jan-63		30-Jan-63	
MAR 1965	23-Mar-65	****		****	
DEC 1965	8-Dec-65	16-Dec-65		18-Dec-65	
FEB 1966	24-Feb-66	23-Feb-66		23-Feb-66	
JAN 1968	****	7-Jan-68		7-Jan-68	
NOV 1968	27-Nov-68	28-Nov-68		29-Nov-68	
MAR 1969	13-Mar-69	13-Mar-69		****	
JAN 1970	2-Jan-70	2-Jan-70		2-Jan-70	
JAN 1971	17-Jan-71	18-Jan-71		18-Jan-71	
MAR 1971	20-Mar-71	20-Mar-71		20-Mar-71	
JAN 1973	2-Feb-73	31-Jan-73		31-Jan-73	
JAN 1977	****	9-Jan-77		9-Jan-77	
FEB 1979	22-Feb-79	22-Feb-79	22-Feb-79	22-Feb-79	
FEB 1980	29-Feb-80	29-Feb-80	29-Feb-80	29-Feb-80	29-Feb-80
FEB 1981	****	****	****	6-Feb-81	****
MAR 1981	****	4-Mar-81	4-Mar-81	4-Mar-81	****
DEC 1981	4-Dec-81	4-Dec-81	4-Dec-81	4-Dec-81	4-Dec-81
FEB 1984	24-Feb-84	24-Feb-84	24-Feb-84	24-Feb-84	24-Feb-84
JAN 1985	2-Jan-85	1-Jan-85	1-Jan-85	1-Jan-85	1-Jan-85
JAN 1987	23-Jan-87	23-Jan-87	23-Jan-87	23-Jan-87	23-Jan-87
DEC 1987	8-Dec-87	8-Dec-87	8-Dec-87	8-Dec-87	8-Dec-87
MAR 1988	14-Mar-88	14-Mar-88	14-Mar-88	14-Mar-88	14-Mar-88
FEB 1989	22-Feb-89	21-Feb-89	21-Feb-89	21-Feb-89	21-Feb-89
DEC 1998	15-Dec-98	15-Dec-98	15-Dec-98	15-Dec-98	15-Dec-98
FEB 1999	25-Feb-99	26-Feb-99	26-Feb-99	26-Feb-99	26-Feb-99
MAR 2000	20-Mar-00	20-Mar-00	20-Mar-00	20-Mar-00	20-Mar-00
FEB 2001	11-Feb-01	11-Feb-01	11-Feb-01	11-Feb-01	11-Feb-01
DEC 2001	2-Jan-02	31-Dec-01	30-Dec-01	31-Dec-01	30-Dec-01
FEB 2002	****	18-Feb-02	****	****	17-Feb-02
JAN 2003	18-Jan-03		18-Jan-03	18-Jan-03	18-Jan-03
JAN 2004	7-Jan-04		5-Jan-04	5-Jan-04	5-Jan-04
JAN 2006	21-Jan-06		21-Jan-06	21-Jan-06	21-Jan-06
FEB 2007	24-Feb-07		24-Feb-07	24-Feb-07	24-Feb-07

FEB 2008	22-Feb-08	22-Feb-08	22-Feb-08	22-Feb-08
JAN 2009	24-Jan-09	24-Jan-09	24-Jan-09	24-Jan-09
FEB 2010	9-Feb-10	9-Feb-10	9-Feb-10	9-Feb-10
MAR 2010	24-Mar-10	24-Mar-10	24-Mar-10	24-Mar-10
JAN 2013	7-Jan-13	6-Jan-13	7-Jan-13	6-Jan-13